Determination of the stable iron isotopic composition of sequentially leached iron phases in marine sediments

Susann Henkel[1,2], Sabine Kasten[2], Simon W. Poulton[3], and Michael Staubwasser[1]

[1] University of Cologne, Zülpicher Str. 49a, 50674 Cologne, Germany

[2] Alfred Wegener Institute, Helmholtz Centre for Polar and Marine Research, Am Handelshafen 12, 27570 Bremerhaven, Germany

[3] School of Earth and Environment, The University of Leeds, Leeds, LS2 9JT, United Kingdom

Corresponding author: Susann Henkel (susann.henkel@awi.de)

Abstract

Reactive iron (oxyhydr)oxide minerals preferentially undergo early diagenetic redox cycling which can result in the production of dissolved Fe(II), adsorption of Fe(II) onto particle surfaces, and the formation of authigenic Fe minerals. The partitioning of iron in sediments has traditionally been studied by applying sequential extractions that target operationally-defined iron phases. Here, we complement an existing sequential leaching method by developing a sample processing protocol for δ^{56}Fe analysis, which we subsequently use to study Fe phase-specific fractionation related to dissimilatory iron reduction in a modern marine sediment. Carbonate-Fe was extracted by acetate, easily reducible oxides (e.g. ferrihydrite and lepidocrocite) by hydroxylamine-HCl, reducible oxides (e.g. goethite and hematite) by dithionite-citrate, and magnetite by ammonium oxalate. Subsequently, the samples were repeatedly oxidized, heated and purified via Fe precipitation and column

chromatography. The method was applied to surface sediments collected from the North Sea, south of the Island of Helgoland. The acetate-soluble fraction (targeting siderite and ankerite) showed a pronounced downcore δ^{56}Fe trend. This iron pool was most depleted in ^{56}Fe close to the sediment-water interface, similar to trends observed for pore-water Fe(II). We interpret this pool as surface-reduced Fe(II), rather than siderite or ankerite, that was open to electron and atom exchange with the oxide surface. Common extractions using 0.5 M HCl or Na-dithionite alone may not resolve such trends, as they dissolve iron from isotopically distinct pools leading to a mixed signal. Na-dithionite leaching alone, for example, targets the sum of reducible Fe oxides that potentially differ in their isotopic fingerprint. Hence, the development of a sequential extraction Fe isotope protocol provides a new opportunity for detailed study of the behavior of iron in a wide-range of environmental settings.

Keywords

Iron, sediment, sequential extraction, stable Fe isotopes, early diagenesis

1 Introduction

The many aspects of the biogeochemical cycle of Fe, such as sources and sinks, changes in redox state, and phase transformations have been intensely studied in continental and marine environments. Iron fluxes and the bioavailability of respective Fe mineral phases, however, are still poorly constrained (Raiswell and Canfield 2012), mainly due to methodological challenges in tracing the complex reaction pathways in which Fe participates. As early as the 1960s and 1970s, the need for separation of (highly) reactive Fe minerals from unreactive phases led to the development of sequential chemical extraction methods (e.g. Mehra and Jackson 1960, Schwertmann 1964, McKeague and Day 1966, Tessier et al. 1979).

Since then these schemes have been modified to enhance their selectivity (e.g. Lord III 1980, Phillips and Lovley 1987, Cornwell and Morse 1987, Ferdelman 1988, Canfield 1988, Kostka and Luther 1994, Haese et al. 1997, Hyacinthe and Van Capellen 2004, Poulton and Canfield 2005, Raiswell et al. 2010). Although operationally-defined and not entirely mineral-specific, these methods are now routinely applied in soil and sediment biogeochemical studies. In soil science, Fe solid phase speciation and distribution patterns are used to classify soils and to reconstruct pedogenesis (e.g. Wiederhold et al. 2007a). Soil Fe mineralogy has been shown to control the mobility of pollutants and other nutrients (Stucki et al. 1988).

Fe extractions in modern marine sediments have often been performed to identify the pool of Fe that is potentially reducible during early diagenesis, either through dissimilatory iron reduction (DIR) (e.g. Slomp et al. 1997, Jensen et al. 2003), or by direct abiotic reduction with dissolved sulphide (e.g. Canfield et al. 1992, Poulton et al. 2004). These extraction procedures have also widely been used to study and quantify the post-depositional alteration of the primary Fe mineral assemblage – including the overprint of rock magnetic characteristics of sediments (e.g. Kasten et al. 1998, Riedinger et al. 2005, März et al. 2008). Furthermore, reactive Fe oxide minerals buried and preserved in subsurface marine sediments have recently been suggested to be an important substrate in the anaerobic oxidation of methane (e.g. Beal et al. 2009, Segarra et al. 2013, Riedinger et al. 2014, Sivan et al. 2011, 2014, Egger et al. 2015). Similarly, for ancient sediments, the analysis of sequentially leached solid phase iron species in black shales and banded iron formations, has revealed important insight into the redox-state of the past ocean (e.g. Poulton and Canfield 2011).

A growing number of studies on Fe sources to the ocean, and reaction pathways in the modern or ancient marine environment, have focused on, or have been complemented by, stable Fe isotope analysis (e.g. Anbar and Rouxel 2007, Johnson et al. 2008, Conway and John

2014). In particular, biologically-driven redox cycling initiated by DIR may lead to a specific Fe isotope compositional fingerprint, which distinguishes such Fe from other sources, such as hydrothermal fluids, river discharge, and dust deposition (Beard et al. 2003a, Severmann et al. 2010, Homoky et al. 2009, 2013). However, experimental studies – biotic and abiotic – demonstrate the complexity of Fe isotope fractionation during specific reaction pathways and between the Fe mineral phases involved. For example, isotope fractionation occurs between dissolved Fe, surface-bound Fe, and the bulk of the Fe-oxide mineral during both DIR (Crosby et al. 2007) and abiotic equilibrium exchange (Wu et al. 2011). During pyrite formation, Fe isotopes fractionate between dissolved Fe, mackinawite, and pyrite (Guilbaud et al. 2013). The use of Fe isotopes as a fingerprint for a specific source or reaction pathway may therefore require analytical discrimination between different Fe phases.

Sequential leaching techniques may provide the means to address the above isotopic complexity. Initial studies have shown, for example, that the isotopic fingerprint of DIR in marine sediments is detectable only in the reactive Fe oxides (Severmann et al. 2006, Staubwasser et al. 2006). Similarly, the first Fe isotope data obtained from partial selective leaching of soils has provided valuable insight into the weathering of Fe minerals and their utilization as nutrient sources during plant growth (Wiederhold 2007b, Guelke et al. 2010). In an attempt to address Fe fluxes to the ocean, Scholz et al. (2014) used Fe concentration data from sequential leaching extracts, in combination with Fe isotope data from HCl leaching, to identify diagenetic Fe recycling into the water column on the eastern Pacific margin. The logic next step is to apply Fe isotope analyses directly to a full sequential leaching protocol. However, there are a number of analytical issues that must be solved prior to application, such as potential isotope fractionation during the Fe separation chemistry required for isotope

96 analysis, and matrix-induced mass bias from residual leaching chemicals during mass
97 spectrometry.

98 Here, we have developed a protocol to measure Fe isotopes in different operationally-
99 defined Fe pools targeted by a commonly used extraction procedure for modern and ancient
100 sediments (Poulton and Canfield 2005; henceforth referred to as the PC-Method). The method
101 was developed mainly to study the redox evolution of depositional environments recorded in
102 sedimentary archives, but is more broadly applicable to studies of Fe biogeochemistry in
103 modern and ancient settings. The PC-Method targets a variety of ´highly reactive´ Fe phases,
104 including carbonate Fe (e.g. siderite) with acetic acid, easily reducible Fe hydroxides and
105 oxyhydroxides (ferrihydrite, lepidocrocite) with hydroxylamine-HCl, reducible (oxyhydr)oxides
106 (goethite, hematite, akaganéite) with a solution of Na-dithionite and Na-citrate, and
107 magnetite with oxalic acid. Some of these leaching steps have been applied in earlier Fe
108 isotope studies of recent sediments (Staubwasser et al. 2006) and soils (Wiederhold et al.
109 2007a, 2007b, Guelke et al. 2010), but the full sequential scheme has not previously been
110 applied to Fe isotope studies. The PC-Method includes a separate chromous chloride
111 reduction of FeS_2, but this technique extracts other Fe phases as well, and is also unsuitable
112 for Fe isotope analysis because of a mass interference of ^{54}Cr on ^{54}Fe, which cannot be
113 corrected for if Cr is present above typical blank concentrations during mass spectrometry. A
114 better method for extracting silicates (with HF) and pyrite (HF-insoluble residue) was
115 developed by Huerta-Diaz and Morse (1990) and adopted for iron isotope analysis by
116 Severmann et al. (2006). This approach may be used subsequently to the extraction protocol
117 shown here, to determine the isotopic composition of pyrite Fe.

118

119

2 Method development and testing

2.1 Extraction of Fe phases (PC-Method)

Leaching is generally started with 5 mL of 1 M Na-acetate (adjusted to pH 4.5 with acetic acid) per ~50 mg of sediment for 24 h under an Ar-atmosphere. This extraction step targets carbonate-associated Fe (Tessier et al. 1979, Poulton and Canfield 2005), but also removes AVS (Cornwell and Morse 1987, Poulton and Canfield 2005) and surface-reduced Fe(II) (Crosby et al. 2005, 2007). In the second step, 5 mL of 1 M hydroxylamine-HCl in 25% v/v acetic acid (Chester and Hughes 1967) are reacted with the residue for 48 h. This step targets easily reducible Fe oxide minerals such as ferrihydrite and lepidocrocite (Poulton and Canfield 2005). Leaching is then continued with a 2 h treatment of 5 mL of Na-dithionite (50 g L^{-1})/Na-citrate solution (pH 4.8) (Mehra and Jackson 1960, Lord III 1980). Compared to Canfield (1989) and Poulton and Canfield (2005) we used less citrate (0.02 M instead of 0.2 M) in order to lower the risk of matrix effects during MC-ICP-MS measurements. Citrate is commonly added as a complexing agent in excess to complex Fe(II) in solution. We ensured the stability of Fe in solution by performing this extraction step under anoxic conditions and observed total dissolution of a goethite-hematite mineral standard (see below) and no re-precipitation of Fe (oxyhydr)oxides. The sequential extraction is completed by leaching with 0.2 M ammonium oxalate/0.17 M oxalic acid for 6 h to dissolve magnetite. After each extraction step samples were centrifuged and the supernatants filtered through 0.2 µm polyethersulfone filters.

2.2 Preparation of leachate solutions for isotope analysis

The PC-Method was modified to accommodate the requirements for δ^{56}Fe isotope analysis, where the main problem is uncorrectable matrix-induced bias of measured isotope ratios. Procedures were developed to remove the leaching chemicals prior to standard column

144 chromatography and mass-spectrometric methods (see below). The matrix removal and the
145 accuracies of isotope ratios were verified by reference samples of known composition. These
146 were a) 0.5 mL of an iron standard solution (1000 ppm Fe Certipur®) to which for each leaching
147 step the appropriate chemicals were added and subsequently removed, and b) a hematite-
148 goethite mixture prepared according to Cornell and Schwertmann (1996) (δ^{56}Fe: 0.26±0.03‰,
149 see Staubwasser et al. 2006), which was used for the dithionite extraction step only. These
150 and all other subsequent (natural and artificial) samples were processed as follows:

151 *Acetate extraction, (Fe_{aca}):* After centrifugation and filtration the acetate matrix was destroyed
152 by repetitive oxidation in a mixture of distilled HNO_3 and HCl (1:3) with additional H_2O_2 (supra
153 pure grade) (see below for reproducibility of $\delta^{56}Fe_{Fe_{aca}}$ data). The complete procedure for
154 matrix removal is shown in Figure 1. Iron was precipitated from the solution as Fe hydroxide
155 (Fig. 1) to ensure complete separation from matrix. (Centrifuging the samples at 4°C helps to
156 keep the Fe precipitate at the bottom of the test tube.) Subsequently, column
157 chromatography was performed using the BioRad AG® 1-X8 anion exchange resin (Strelow
158 1980), as described by Schoenberg and von Blanckenburg (2005).

159 *Hydroxylamine-HCl extraction (Fe_{hyam}):* Filtered samples were repetitively oxidized and re-
160 dissolved in 6 M HCl before column separation was performed as described for the previous
161 extraction step (Fig. 1).

162 *Na-dithionite/Na-citrate extraction ($Fe_{di\text{-}ct}$):* Samples were oxidized (Fig. 1) and after
163 evaporation, residues were heated for >7 h at 190°C for thermal destruction of the citrate.
164 Afterwards, H_2O_2 and *aqua regia* were carefully added to the samples to oxidize the reduced
165 sulfur species in the remaining dithionite to SO_4^{2-}. Subsequent iron hydroxide precipitation
166 (Fig. 1) was performed to remove all Fe from the sulfate matrix which would otherwise

overload the anion exchange resin. Furthermore, iron precipitation showed whether citrate was fully removed from the solution, whereby incomplete iron precipitation was indicated by a yellowish supernatant color due to citrate remaining in the solution. In this case, thermal heating was repeated. Further processing of the samples for column chromatography was performed as described above.

Oxalic acid extraction (Fe_{oxa}): The filtrate was oxidized and after evaporation, samples were heated for 24 h at 140°C to further oxidize the oxalate to CO_2 (Fig. 1). During heating, oxalate crystals condensating at the rim of the beakers were flushed back with ultra-pure water. Residues were re-dissolved in *aqua regia* and H_2O_2 (Fig. 1). After boiling (2 h at 120°C) and evaporation, iron precipitation and sample preparation for column chromatography was performed as described above. Iron precipitation was performed to ensure the completeness of oxalate removal. When Fe precipitation was inhibited, heating of the sample for oxalate destruction was repeated.

2.3 MC-ICP-MS setup

Prior to mass-spectrometry, concentrations of leached sediment samples were matched to 1 ppm following ICP-OES analysis (Spectro Arcos ICP-OES). Iron isotope measurements were performed on a ThermoFinnigan Neptune MC-ICP-MS instrument at the Steinmann Institute in Bonn following the method described by Schoenberg and von Blanckenburg (2005). ^{53}Cr and ^{60}Ni were simultaneously measured to monitor interferences of ^{54}Cr on ^{54}Fe and ^{58}Ni on ^{58}Fe, and the data corrected accordingly. We used the standard-sample bracketing method with the IRMM-014 standard. An in-house standard (Johnson&Matthey, Fe Puratronic wire, $\delta^{56}Fe = 0.42 \pm 0.05‰$) was additionally measured every

6 samples to monitor accuracy. Pore-water samples were matched to 0.2 ppm and measured using an ESI Apex-Q desolvator instead of the regular glass spray chamber.

Data are reported as

$$\delta^{56}Fe\ [‰] = [(^{56}Fe/^{54}Fe_{sample}) / (^{56}Fe/^{54}Fe_{IRMM\text{-}014}) - 1] * 1000$$

Iron isotope fractionation between two species X and Y are given as

$$\Delta^{56}Fe_{X\text{-}Y} = \delta^{56}Fe_X - \delta^{56}Fe_Y$$

2.4 Procedure blanks, accuracy and reproducibility of δ^{56}Fe data leached from sediment samples

Recoveries of the Certipur® Fe standards were between 83 and 101% for all extractants, when normalized to the unprocessed standard solution (Table 1). The amount of Fe in the standards (0.5 mg) was higher, but in the same order of magnitude as that extracted from sediments. The low recoveries for oxalate are due to loss of material during the sometimes vigorous oxidation reaction. Reagent blanks were 1.2 ng mL^{-1} for Na acetate solution, 43 ng mL^{-1} for hydroxylamine-HCl, 54 ng mL^{-1} for dithionite-citrate, and 4.1 ng mL^{-1} for oxalate. Processing blanks that were added in between sediment samples had between 0.1 and 0.4 µg Fe (Table 1) and were thus two to three orders of magnitude lower than Fe contents of natural samples. Three out of 33 blanks were clearly contaminated (Grubb's outlier test, α=0.05) and therefore eliminated from calculations. Contamination concerned oxalate samples and may have happened during the thermal destruction step.

The Certipur® standards that underwent chemical processing were isotopically identical within error to the unprocessed solution (δ^{56}Fe = 0.15±0.03‰, n=9). Values for the extractants were: 0.14±0.03‰ for acetate (n=7), 0.13±0.02‰ for hydroxylamine-HCl (n=5),

213 0.09±0.03‰ for dithionite-citrate (n=7), and 0.14±0.04‰ for oxalate (n=5) (Fig. 2). The
214 reproducibility of our internal Certipur® standard, regardless of whether it was subjected to
215 the extraction steps of the PC-Method or not, suggests that the process that led to the loss of
216 Fe during processing of the samples did not result in a significant fractionation of Fe isotopes.
217 The hematite-goethite standard was also dissolved in HCl/HNO_3 and measured without
218 further chemical treatment, except for the column separation. This gave a $\delta^{56}Fe$ composition
219 of 0.27±0.01‰ (1SD, n=3, Fig. 2). The $\delta^{56}Fe$ value of the dithionite-leached and fully processed
220 mineral standards was 0.30±0.07‰ (n=5) compared to 0.26±0.03‰ given by Staubwasser et
221 al. (2006) (n=11). These data demonstrate the absence of matrix-induced bias in Fe isotope
222 ratios in samples leached and subsequently processed by the methods outlined in this study.

223

224 **2.5 Selectivity of the Fe extraction steps**

225 **2.5.1 Materials and set-up of experiments**

226 *Time resolved leaching rate experiments:* Using synthetic minerals, the selectivity of the
227 chemical extractions by Na-acetate, hydroxylamine-HCl, and Na-dithionite/Na-citrate was
228 evaluated. This is important, as dependent on the size of Fe pools and their isotopic
229 differences, non-selectivity of the leaching can lead to incorrect Fe isotope values for the
230 actual target fraction. The minerals were synthesized after Cornell and Schwertmann (1996).
231 About 5 mg of the specific Fe oxide was suspended in 50 mL of an extraction solution not
232 designed to lead to its dissolution: ferrihydrite was treated with Na-acetate for 12, 24, 36, 48,
233 and 60 h, goethite and hematite were treated with hydroxylamine-HCl for 12, 24, 36, 48, and
234 60 h, and magnetite was treated with Na-dithionite/Na-citrate for 1, 2, and 4 h. In contrast to
235 earlier studies (Canfield 1988, Raiswell et al. 1994, Poulton and Canfield 2005) magnetite was

236 significantly dissolved by dithionite treatment (see below) and the leaching was thus repeated
237 using magnetite purchased from Alfa Aesar. Although not used on natural samples in this
238 study, we also evaluated 0.5 M HCl extraction that targets poorly crystalline hydrous ferric
239 oxides such as ferrihydrite (Kosta and Luther 1994, Severmann et al. 2006). The synthetic
240 minerals ferrihydrite, goethite, hematite, and magnetite were subject to 0.5 M HCl for 0.5, 1,
241 2, 4, and 8 h at room temperature. After each time step, the respective samples were
242 centrifuged and aliquots of 15 mL were filtered. Na-acetate, hydroxylamine-HCl, and
243 dithionite samples were processed as described above, but omitting Fe precipitation and
244 column chromatography as only Fe concentrations were to be obtained. The processing of
245 HCl-samples was reduced to evaporation and subsequent re-dissolution in 0.3 M HNO_3 prior
246 to Fe concentration measurement by ICP-OES.

247 *Leaching of pairs of isotopically spiked and non-spiked minerals:* Mixtures of two synthetic
248 minerals were treated with extractants (hydroxylamine-HCl, Na-dithionite, and 0.5 M HCl) to
249 test the selectivity of the leaching steps. The respective target mineral was mixed with a ^{58}Fe-
250 spiked non-target mineral (e.g. non-spiked ferrihydrite plus spiked goethite for
251 hydroxylamine-HCl extraction). Based on the aforementioned observation of our magnetite
252 minerals significantly dissolving in dithionite solution, additional tests with magnetite
253 purchased from Alfa Aesar (non-spiked) were performed with spiked goethite and hematite,
254 respectively. To allow for the high iron concentrations when using pure phases compared to
255 natural sediment samples, about 10 mg of the synthetic minerals (5 mg spiked mineral + 5 mg
256 non-spiked mineral) was treated with 50 mL of the respective leaching reagent (in contrast to
257 50 mg + 5 mL for sediment samples, see above). For each mineral pair, three replicates were
258 processed. After centrifugation, 15 mL of the extract was filtered for further processing for Fe
259 isotope analysis as described above. Dissolution of target and non-target minerals was

evaluated by comparing $^{58}Fe/^{54}Fe$ ratios of the leachates with those of the respective pure synthetic minerals. The latter ratios were determined after dissolution of the pure minerals in *aqua regia*, evaporation, re-dissolution in 6 M HCl, and column chromatography.

2.5.2 Selectivity of extraction steps

Time resolved leaching rate experiments: With the exception of the dithionite extraction, the treatment of synthetic Fe (oxyhydr)oxide minerals with reagents that are commonly used in the subsequent extraction step led to only minor dissolution, verifying the results of Poulton and Canfield (2005). As expected, mineral dissolution increased with the duration of leaching (Fig. 3). At optimum times for acetate- and hydroxylamine-HCl extractions (according to the PC-Method), less than 1% of the non-target minerals ferrihydrite and goethite + hematite, respectively, were dissolved. Carry-over of ferrihydrite-Fe into the Na-acetate fraction was 0.3% compared to 1.7% given by Poulton and Canfield (2005) and can thus be considered insignificant. The slightly higher dissolution of hematite in hydroxylamine-HCl compared to goethite could be related to grain-size differences and also the degree of crystallinity of the hematite (freshly-precipitated hematite is more readily dissolved than natural hematite; Raiswell et al. 1994). With respect to iron isotope signatures, a carry-over of <1% of goethite- and hematite-Fe into the fraction of amorphous Fe is, however, insignificant for typical marine or fluvial sediments as Fe_{hyam} and $Fe_{di\text{-}ct}$ concentrations usually range in the same order of magnitude.

We observed considerable dissolution of magnetite in Na-dithionite/Na-citrate for both the magnetite synthesized after Cornell and Schwertmann (1996) and the magnetite purchased from Alfa Aesar. The 2 h-treatment led to dissolution of up to 50% of the magnetite (Fig. 3), which is in contrast to the results of Poulton and Canfield (2005) who observed

dissolution of only up to 7%, and Raiswell et al. (1994) who observed only 4% dissolution. In our study the significant difference in dissolution of the magnetite produced after Cornell and Schwertmann (1996) and the purchased magnetite (52% vs. 32% after 2 h in dithionite/citrate) indicates that grain size might considerably affect dissolution. However, the magnetite synthesized after Cornell & Schwertmann was similar to that used by Poulton and Canfield (2005) and yet was strongly dissolved. Interestingly, Kostka and Luther (1994) also observed significant magnetite dissolution in dithionite (90.2%). The authors, however, leached for 4 h at 60°C, so their data are not directly comparable to previous studies. The disparity in our data relative to previous studies was possibly caused by differences in sample size used per volume of solution, crystallinity, or potentially by partial oxidation of magnetite during storage. The 1 h extraction by 0.5 M HCl resulted in effective dissolution of ferrihydrite (>95%) while goethite, hematite, and magnetite remained largely unaffected (Fig. 3).

Leaching of pairs of isotopically spiked and non-spiked minerals: Test results of experiments with ^{58}Fe spiked and non-spiked minerals are shown in Table 2. The ^{58}Fe/^{54}Fe ratios of samples and pure minerals as end-members are given in the appendix (Tables A.1 and A.2). In accordance with the previous time-resolved experiment, the isotopic data of leached mineral mixtures demonstrate that goethite and hematite remain unaffected by the hydroxylamine-HCl extraction. For both pairs (each with ferrihydrite), 98% of the dissolved Fe in solution was derived from ferrihydrite and ~2% originated from goethite and hematite. In hydroxylamine-HCl, 87% of the ferrihydrite-Fe was recovered, which is slightly less than the 99% given by Poulton and Canfield (2005). Dithionite effectively dissolved goethite and hematite. In the first experiment, where minerals have been mixed with ^{58}Fe-spiked magnetite synthesized after Cornell and Schwertmann (1996), ~96% of goethite and hematite were dissolved after 2 h. In the repeated run with magnetite from Alfa Aesar, recoveries were,

however, lower (79 to 88%; Table 2). In both runs, magnetite was significantly dissolved and data produced by the mixing experiment match those of the single mineral extraction: Dithionite extracted up to 50-60% of our synthetic magnetite and 30-40% of the Alfa Aesar magnetite.

3 Application of the new method to surface sediments of the North Sea

3.1 Material and methods

3.1.1 Core location and sampling

Data presented in this study were obtained for surface sediments retrieved by a multicorer in the German Bight (North Sea, 54°5.06' N, 7°54.94' E, 36 m water depth; site HE337-1) in 2010 during cruise HE337 of research vessel HEINCKE. The sediment cores were collected west of the so-called Helgoland mud area, one of the few depocenters of fine-grained sediments in the North Sea with eddy focusing of fine-grained material from the rivers Weser and Ems (Hertweck 1983). Sedimentation rates in the Helgoland mud area are ~2.6 mm/yr for the last 750 years (Hebbeln et al. 2003). The location was chosen as sediments exhibit an extended ferruginous zone starting directly below the sediment surface in contrast to deposits within the Helgoland mud area proper, where the upper iron reduction zone is limited to the upper 15 cm (Oni et al. 2015). At the core location, bioturbation (and potentially bioirrigation) occur. However, the generally rather undisturbed pore-water profiles suggest that these processes proceed at a comparatively low rate (see section 3.2).

Sediment analyses performed on one core included the sequential iron extractions of the PC-Method for iron concentration and iron isotope analysis, bulk sediment total acid digestion for total Al, Mn, and Fe (Fe_{total}) contents, in addition to AVS and pyrite-sulfide extraction after Canfield et al. (1986) (without subsequent Fe isotope analysis). Sediment was

332 sampled directly on board using syringes with cut tips. The syringes were sealed and stored in
333 Ar-filled gas-tight glass containers at -20°C until processing to prevent secondary mineral
334 precipitation. Pore-water was sampled from a parallel core using rhizons (Seeberg-Elverfeldt
335 et al. 2005, Dickens et al. 2007) that were inserted into pre-drilled holes in the liner. In order
336 to inhibit oxidation during sampling, due to O_2 in either the rhizon or the attached syringe, the
337 rhizons were pre-soaked with ultra-pure water and the first 0.5 mL or pore-water was
338 discarded. Pore-water aliquots for $\delta^{56}Fe_{Fe(II)_{aq}}$ were acidified with double distilled HCl and
339 stored in pre-cleaned vials at 4°C.

340

341 **3.1.2 Sequential Fe extraction (PC-Method)**

342 Sediment samples were leached in random order. About 50 mg of freeze-dried
343 sediment was washed with 5 mL of 1 M $MgCl_2$ for 2 h in order to remove pore-water
344 constituents, which will also have removed exchangeable ions on particle surfaces (Tessier et
345 al. 1979, Poulton and Canfield 2005). The $MgCl_2$ washing was performed under an Ar
346 atmosphere to prevent oxidation. The residue was then used for the subsequent extraction
347 steps (see chapter 2.1). The extraction solutions were processed as described in sections 2.2
348 and 2.3.

349

350 **3.1.3 Bulk sediment composition**

351 Total acid digestion of sediment samples was performed with a CEM Mars Xpress
352 microwave system using ~50 mg of freeze-dried sediment and a mixture of HNO_3 (3 mL), HCl
353 (2 mL), and HF (0.5 mL). With each set of samples, blanks and standard reference material

354 (NIST SRM 2702) were processed. Element concentrations were measured by ICP-OES (Iris
355 Intreprid II). Recoveries of the standard were 97.5% for Al, 100.4% for Fe, and 98.9% for Mn.

356

357 **3.1.4 AVS- and pyrite-S**

358 Acid volatile sulfide and pyrite were determined for the North Sea sediments to both
359 correct the Na-acetate leached Fe pool for the presence of AVS, and to assess the extent of
360 early diagenetic iron transformation at the study site. Extractions (after Canfield et al. 1986)
361 with HCl (for AVS) and chromous chloride distillation (for pyrite) were performed at the
362 University of Leeds. These extractions determine the concentration of sulfide present, which
363 is then stoichiometrically converted to the appropriate Fe concentration. Replicates of three
364 samples (each analyzed 2-4 times) revealed good reproducibility with a RSD of below 5% in all
365 cases. Accuracy was evaluated by analysis of an in-house standard (HN22) with a pyrite-Fe
366 content of 2.12 ± 0.16 wt% (our measured value: 2.18 wt%).

367

368 **3.1.5 Pore-water composition**

369 On board pore-water analyses comprised the determination of $Fe(II)_{aq}$ using the
370 ferrozine method of Stookey (1970) and of alkalinity by titration with HCl (see appendix A.3
371 for alkalinity). Offshore measurements of SO_4^{2-} were performed as described by Henkel et al.
372 (2012). Pore-water Fe for $\delta^{56}Fe_{Fe(II)_{aq}}$ analysis was concentrated and purified from anions using
373 NTA Superflow (Lohan et al. 2005). The acidified samples were titrated with NH_4OH (supra
374 pure grade) to a final pH of 2. In order to oxidize Fe(II) to Fe(III), 10 µM H_2O_2 was added to the
375 samples before loading of NTA Superflow columns (Qiagen). The NTA columns were pre-
376 conditioned with HCl (pH2, HCl triple distilled). Fe was subsequently eluted using 1 M HCl. The

samples were further purified by anion exchange chromatography as described in section 2.2 and measured by MC-ICP-MS (see section 2.3).

3.2 Results and discussion

3.2.1 Geochemical results

Geochemical data gained for Site HE337-1, including Fe phases and pore-water constituents are shown in Figures 4 and 5 (note that Fe_{aca}* has been corrected for Fe_{AVS} and that Fe_{AVS} was a minor constituent of Fe_{aca} in our samples; Figure 5). Total Fe contents range between 1.9 and 4.6 wt%. Unsulfidized reactive iron (Fe_{unsulf} =Fe_{aca}*+ Fe_{hyam} + $Fe_{di\text{-}ct}$ + Fe_{ox}) varies between 0.5 and 1.0 wt% (Fig. 4). Although Fe_{unsulf} remains relatively constant with depth, a decrease in Fe_{unsulf} relative to Fe_{total} is observed with depth through the top 10 cm of the sediment. At the core top, Fe_{hyam} represents about 50% of the unsulfidized Fe pool, and when normalized to Fe_{unsulf}, shows an overall decrease to ~20 cm depth (Fig. 5). Fe_{aca} and $Fe_{di\text{-}ct}$ amount to ~20 and ~30% of Fe_{unsulf}, respectively. Whereas Fe_{aca}/Fe_{unsulf} generally increases towards 20 cm depth, with a subsequent overall decrease below, albeit with significant variability at certain horizons, $Fe_{di\text{-}ct}/Fe_{unsulf}$ does not show a clear trend with depth. Fe_{oxa} is of minor importance, contributing only ~10% to the Fe_{unsulf} pool throughout most of the core, perhaps with a slight increase in Fe_{oxa}/Fe_{unsulf} over the top 10 cm. Regarding the generally lower amount of Fe_{oxa} compared to $Fe_{di\text{-}ct}$ in this core, we consider the effect of any possible magnetite dissolution in the $Fe_{di\text{-}ct}$ extract as being minor.

Sulfide-bound Fe is mainly present as pyrite (Fig. 5) with an increase towards 15 cm depth. The Fe_{AVS} pool is relatively insignificant, with highest contents of 0.02 wt% at 18 cm depth. Manganese oxide reduction is evidenced by a pronounced Mn/Al decrease in the top 3 cm (Fig. 4). Pore-water profiles (Fig. 4) indicate organoclastic sulfate reduction at ~7 cm

depth coinciding with a peak in $Fe(II)_{aq}$ (~200 µM) produced by DIR, with ferruginous pore-water prevailing over the full length of the core. $\delta^{56}Fe_{Fe_{aq}}$ values are lightest (-1.3‰) at 1.5 and 4.5 cm depth, where DIR dominates Fe cycling. At 0.5 cm, where Fe(II) is removed from solution by oxidative precipitation (as indicated by a drawdown of $Fe(II)_{aq}$), $\delta^{56}Fe_{Fe_{aq}}$ is slightly heavier (-0.9‰). Below 5 cm depth (still within the $Fe(II)_{aq}$ maximum and coinciding with the presence of AVS), the isotopic composition of pore-water Fe becomes heavier and reaches a value of about zero at 18 cm, where $Fe(II)_{aq}$ concentrations level off to about 40 µM.

In the leached sediment fractions, a pronounced $\delta^{56}Fe$ trend with depth is observed only for Fe_{aca}, with values that increase from ~-1‰ at the surface, to slightly positive values at depth (Fig. 5). Fe_{hyam} shows an overall depletion in ^{56}Fe ($\delta^{56}Fe$ = -0.38±0.11‰), whereas $Fe_{di\text{-}ct}$ and Fe_{oxa} show near zero values (-0.07±0.09‰ and -0.15±0.08‰, respectively).

3.2.2 Early diagenetic iron cycling in shallow North Sea sediments

The Fe phases extracted by the dithionite/citrate and oxalate solutions (goethite, hematite, magnetite) are largely unaffected by DIR as concluded from the absence of clear downcore trends in $Fe_{di\text{-}ct}$ and Fe_{oxa} contents and respective $\delta^{56}Fe$ profiles (Fig. 5). Near zero values of $\delta^{56}Fe_{di\text{-}ct}$ and $\delta^{56}Fe_{oxa}$ reflect largely unaltered terrigenous input of these fractions (e.g. Johnson et al. 2008). $Fe_{di\text{-}ct}$ and Fe_{oxa} contents vary between 0.1 to 0.3 wt% and 0.03 to 0.09 wt%, respectively (see appendix A.4). The downcore variability in $Fe_{di\text{-}ct}/Fe_{react}$ and Fe_{oxa}/Fe_{react} is most likely related to changing depositional regimes/sediment accumulation, rather than to a diagenetic overprint. As has been pointed out by Hebbeln et al. (2003), the intensification of beam-trawl fishing off the German coast increased overall sediment accumulation in the mud area during the 20th century and led to a coarsening of sediments.

These changes caused by anthropogenic activity are likely also reflected at Site HE337-1. Here, west of the mud area, sedimentation rates are expected to be lower than the ~2.6 mm/yr in the sediment-focusing mud area (Hebbeln et al. 2003). Consequently, the retrieved sediment core covers at least the past 150 yrs and thus the time when sedimentation patterns changed.

The slight ^{56}Fe-depletion in the hydroxylamine-leachable fraction ($\delta^{56}Fe_{hyam} \approx$ -0.38‰), relative to terrigenous sediments typically showing similar δ^{56}Fe values to igneous rocks (~0.1‰; Beard et al. 2003b) might reflect that part of the pool was diagenetically altered by precipitation of secondary amorphous Fe oxides in the (sub)oxic zone. Under anoxic conditions (below 1-2 cm depth), this pool is used for DIR reflected by a decrease of Fe_{hyam}/Fe_{unsulf} from 0.45 to 0.35 in the top 10 cm (Fig. 5). However, at this location, the Fe_{hyam} reduction does not lead to a significant downcore trend in $\delta^{56}Fe_{hyam}$.

AVS was detected at 3 cm depth, suggesting that sulfidization starts at this depth, which matches the slight SO_4^{2-}-drawdown (Fig. 4). Pyrite, however, is already present in the surface sediment. Bioturbation might have transported iron sulfides previously formed in the deeper part of the sediments towards the sediment surface. There, AVS is prone to oxidation whereas pyrite is less susceptible to oxidation and survives longer before being buried again into the anoxic zone.

The $\delta^{56}Fe_{Fe_{aq}}$ trend towards a slightly heavier value of -0.9‰ at 0.5 cm compared to -1.3‰ at 1.5 cm and at 4.5 cm, where DIR dominates, is explained by oxidative precipitation of Fe that preferentially removes light Fe isotopes (Staubwasser et al. 2013). Since the water column above the sediment is fully oxic, Fe-oxides must precipitate at the sediment surface. The oxidative layer, however, only extents to about 1 cm. Directly below, DIR dominates as indicated by the low $\delta^{56}Fe_{Fe_{aq}}$. Below 5 cm, and in the sample at 3.5 cm, $\delta^{56}Fe_{Fe_{aq}}$ is only -

0.4‰. We suggest that at these depths, AVS formation removes light Fe isotopes from solution. The sediment core was significantly bioturbated and the 3.5 cm sample might reflect local AVS formation in a burrow with elevated TOC contents. Since the $Fe(II)_{aq}$ profile suggests maximum rates of DIR at about 6 cm, DIR and AVS formation seem to coincide at least between 3 and 6 cm depth. Below 18 cm, $\delta^{56}Fe_{Fe_{aq}}$ reaches values of about zero suggesting that DIR is no longer significant and Fe diagenesis is dominated by reactions with H_2S.

3.2.3 Acetate-leachable iron fraction

The comparatively high amounts of Fe_{aca} found at site HE337-1 (0.16±0.05 wt%) are unlikely to be due to the presence of siderite or AVS. AVS only accounts for up to 8% of the Fe_{aca} fraction. The depth of the AVS-maximum (17-21 cm), however, coincides with a local minimum in $\delta^{56}Fe_{aca}$, so the low $\delta^{56}Fe_{aca}$ values at these depths might result from dissolution of the ^{56}Fe-depleted amorphous Fe sulfides (Guilbaud et al. 2013) during the Na-acetate extraction. Siderite is generally considered rare in modern shallow organic-rich marine sediment as it is thermodynamically unstable in the presence of H_2S (Haese 2006). Organoclastic sulfate reduction is clearly occurring in these sediments, as indicated by the presence of AVS and the broad ferruginous zone. As such, even though H_2S is quantitatively removed from solution by reaction with Fe minerals (Fig. 4), siderite would not be expected to form in these sediments. Additionally, $\delta^{56}Fe_{Fe(II)_{aq}}$ data support an absence of authigenic siderite formation: Abiotic siderite precipitation is characterized by a preferential uptake of light isotopes from $Fe(II)_{aq}$. The respective fractionation factor given by Wiesli et al. (2004) is $\Delta^{56}Fe_{Fe(II)_{aq}\text{-siderite}} = +0.48\pm0.22‰$. If Fe_{aca} with $\delta^{56}Fe_{Fe_{aca}}$ ranging between -1 and 0‰ (Fig. 5) was mainly derived from authigenic siderite, respective $\delta^{56}Fe_{Fe(II)_{aq}}$ values would need to be

470 between -0.5 and 0.5‰. In the top 10 cm (where DIR dominates) $\delta^{56}Fe_{Fe(II)_{aq}}$ values are,
471 however, light (-0.4 to -1.4‰) compared to $\delta^{56}Fe_{Fe_{aca}}$.

472 The Fe_{aca} extraction does not include $Fe(II)_{aq}$ as this has been removed by washing the
473 samples with 1 M $MgCl_2$ before the sequential extraction. Without performing a washing step,
474 $Fe(II)_{aq}$ would potentially amount to a maximum of ~20 µg/g sediment, corresponding to ~2%
475 of the Fe_{aca} pool. The above considerations exclude siderite, AVS, and $Fe(II)_{aq}$ as forming a
476 significant proportion of the Na-acetate leached fraction. Instead, we suggest that this pool
477 dominantly reflects isotopically light Fe(II) adsorbed to mineral surfaces following DIR (e.g.
478 Beard et al. 2003a, Williams and Scherer 2004, Crosby et al. 2005, 2007, Mikutta et al. 2009),
479 or Fe(II) that has formed at the surface of Fe oxide minerals via direct abiotic reaction with
480 sulfide, but which dissolves only slowly from the mineral surface at circumneutral pH (Poulton
481 2003, Poulton et al. 2004). Crosby et al. (2005, 2007) investigated isotopic fractionation during
482 DIR using synthesized goethite and hematite, and measured acetate-leached $Fe(II)_{sorb}$ with
483 negative $\delta^{56}Fe$ values resembling those of $Fe(II)_{aq}$ ($\Delta^{56}Fe_{Fe(II)_{aq}-Fe(II)_{sorb}}$=-0.87±0.09‰
484 and -0.30±0.08‰ for goethite and hematite, respectively). $Fe(II)_{sorb}$ derives from ^{56}Fe-
485 depleted pore-water and undergoes electron transfer and Fe(II)-Fe(III) atom exchange with a
486 reactive Fe(III) layer on the ferric substrate (Williams and Scherer 2004; Crosby et al. 2005,
487 2007). The oxide surface becomes more and more enriched in ^{56}Fe balancing out the light
488 $Fe(II)_{aq}$ (Crosby et al. 2005, 2007). $Fe(II)_{sorb}$ thus represents an intermediate between the light
489 $Fe(II)_{aq}$ and isotopically heavy reactive Fe(III). The natural sediments investigated here
490 represent a mineralogically much more complex environment. Nevertheless, we observe
491 trends that resemble those shown in laboratory studies. Therefore we suggest that the
492 underlying processes observed are the same and the light $\delta^{56}Fe$ values we measure for the

493 Fe_{aca} pool likely dominantly reflect Fe(II) at the mineral surface that is fractionated by coupled
494 electron and atom exchange.

495 Our data show variations in $\Delta^{56}Fe_{Fe_{aca}-Fe_{hyam}}$ of between -0.7 to 0.6‰, which is distinct
496 from the fractionation factors found by Crosby et al. (2007). Their $\Delta^{56}Fe_{Fe(II)_{sorb}-Fe(III)_{react}}$ is
497 ~-1.75‰ for goethite and -2.65‰ for hematite experiments. However, the processes at our
498 study site take place in an open system with diffusive $Fe(II)_{aq}$ transport, preferential removal
499 of ^{54}Fe from $Fe(II)_{aq}$ by sulfide precipitation, and non-controlled exposure times of ferric
500 minerals to $Fe(II)_{aq}$. In this regard, and due to the fact that Crosby´s fractionation factors only
501 correspond to the reactive Fe(III) layer (not to the whole ferric substrate), the fractionation
502 factors are not directly comparable.

503 The $\delta^{56}Fe$ measurements suggest that of the unsulfidized solid phase Fe pools in
504 modern DIR-dominated marine sediments, the acetate-leachable pool is the most dynamic. A
505 sequential extraction for marine sediments that uses acetate as a first step followed by
506 hydroxylamine-HCl or 0.5 M HCl leaching is thus to be preferred over leaching with Na-
507 dithionite alone. Leaching by Na-dithionite dissolves a mixture of Fe fractions that are
508 otherwise distinct in origin, reactivity, and isotopic composition and does not selectively
509 resolve the pools truly affected by DIR. Similarly, extractions using 0.5 M HCl alone (i.e. not
510 including the Fe_{aca} extraction first) dissolve the total "easily reducible" Fe fraction, which
511 mainly includes three isotopically distinct Fe pools: the light Fe_{aca} pool that has been shown
512 here to mainly comprise surface-reduced Fe(II), unaltered poorly crystalline hydrous ferric
513 oxides such as ferrihydrite, and ^{56}Fe-enriched reactive Fe at the oxide surface (as identified by
514 Williams and Scherer 2004 and Crosby et al. 2005, 2007). Interpretation of the acetate fraction
515 and its isotopic composition, however, can be problematic where a discrimination between

AVS-Fe, surface-reduced Fe(II), and siderite is not possible and where pore-water δ^{56}Fe data are not available.

4 Conclusions

We have developed a procedure to complement an existing sequential extraction method for Fe phases in marine sediment, to enable stable Fe isotope analysis on the leachates. Processing of the samples for matrix removal did not lead to significant Fe isotope fractionation. This new method was applied to surface sediments collected from the southern North Sea that showed an extended ferruginous pore-water zone. In general, the different δ^{56}Fe values of individual reactive Fe pools demonstrates their different genetic origin: ferrihydrite/lepidocrocite showed lowest average δ^{56}Fe values (-0.38±0.11‰) as they likely include authigenic/secondary phases originating from light $Fe(II)_{aq}$ released into the pore-water by DIR. The detrital origin of the goethite/hematite and magnetite fractions was indicated by δ^{56}Fe≈0‰. Goethite, hematite, and magnetite were not considerably involved in early diagenetic Fe cycling at this locality. The δ^{56}Fe data show large downcore δ^{56}Fe variations in the acetate-leachable fraction. This trend could not be explained by AVS-Fe as respective concentrations were too low. Furthermore, diagenetic siderite was excluded as a significant contributor to the acetate-leachable fraction. We conclude that in these sediments the Na-acetate extraction dominantly comprises surface-reduced Fe(II) which shows a downcore isotopic trend similar to that for $Fe(II)_{aq}$. Although more complex to interpret based on the variety of processes that occur in natural sediments, our data are consistent with the previous laboratory results of Crosby et al. (2005, 2007), who showed that $Fe(II)_{sorb}$ is (isotopically) an intermediate between $Fe(II)_{aq}$ and the ferric substrate. Leaching sediments by 0.5 M HCl or Na-dithionite alone would not resolve this. With extraction by 0.5 M HCl, the isotopically light

Fe(II) would be collected together with the ^{56}Fe-enriched reactive Fe(III) layer at the mineral-surface and the unfractionated initial ferric substrate. The combination of sequential Fe extractions and subsequent δ^{56}Fe analyses as performed in this study represents an approach that can be useful for a broad range of scientific questions in ancient and modern environments characterized by severe redox changes or where control mechanisms for mineral formation (biotic vs. abiotic) are not fully understood.

Acknowledgments: We thank J. Scheld, M. Harak, and J. Menges for assistance in the laboratory at the University of Cologne and appreciate the help of Ingrid Stimac (Alfred Wegener Institute) concerning sulfate measurements and assistance during total digestion of bulk sediments. R. Guilbaud is thanked for giving support during AVS and pyrite determinations at the University of Leeds. X-ray diffractions of synthetic minerals were performed by P. Held (University of Cologne). We further acknowledge F. Wombacher for support concerning MC-ICP-MS at the Steinmann Institute in Bonn and Alison McAnena for producing synthetic minerals. Finally, we thank Jeremy Owens and an anonymous reviewer for helpful comments on the manuscript. This study was funded by the German Research Foundation (DFG) within Priority Program 1158 “Antarctic Research with Comparable Investigations in Arctic Sea Ice Areas” and is associated to the IMCOAST project (Impact of climate induced glacial melting on marine coastal systems in the western Antarctic Peninsula region) (grant numbers STA 936/5-1 and KA 2769/3-1). We acknowledge additional funding by the Helmholtz Association (Alfred Wegener Institute, Helmholtz Centre for Polar and Marine Research) in the framework of the research programs PACES I and PACES II. Data of this study are available via the Pangaea database.

References

Anbar, A.D. and O. Rouxel (2007) Metal stable isotopes in paleoceanography. Annual Review of Earth and Planetary Sciences 35, 717–746.

Beard, B.L., C.M. Johnson, J.L. Skulan, K.H. Nealson, L. Cox, and H. Sun (2003a) Application of Fe isotopes to tracing the geochemical and biological cycling of Fe. Chemical Geology 195, 87–117.

Beal, E.J., C.H. House, and V.J. Orphan (2009) Manganese- and iron-dependant marine methane oxidation. Science 325, 184-187.

Beard, B.L., C.M. Johnson, K.L. Von Damm, and R.L. Poulson (2003b) Iron isotope constraints on Fe cycling and mass balance in oxygenated Earth oceans. Geology 31, 629-632.

Canfield, D.E., R. Raiswell, J.T. Westrich, C.M. Reaves and R.A. Berner (1986), The use of chromium reduction in the analysis of reduced inorganic sulfur in sediments and shales. Chemical Geology 54, 149–155.

Canfield, D.E. (1988) Sulfate reduction and the diagenesis of iron in anoxic marine sediments. Ph.D. thesis. Yale University, 248 pp.

Canfield, D.E. (1989) Reactive iron in marine sediments. Geochimimica et Cosmochimica Acta 53(6), 619–632.

Canfield, D.E., R. Raiswell, and S. Bottrell (1992) The reactivity of sedimentary iron minerals towards sulfide. American Journal of Science 292, 659–683.

Chester, R. and M.J. Hughes (1967) A chemical technique for the separation of ferro-manganese minerals, carbonate minerals and adsorbed trace elements from pelagic sediments. Chemical Geology 2, 249–262.

Conway, T.M. and S.G. John (2014) Quantification of dissolved iron sources to the North Atlantic Ocean. Nature 511, 212–215.

Cornell, R.M. and U. Schwertmann (1996) The iron oxides: structure, properties, reactions, occurrences and uses. VCH Publishers, Weinheim, Germany.

Cornwell, J.C. and J.W. Morse (1987) The characterization of iron sulfide minerals in anoxic marine sediments. Marine Chemistry 22, 193–206.

Crosby, H.A., C.M. Johnson, E.E. Roden, and B.L. Beard (2005) Coupled Fe(II)-Fe(III) electron and atom exchange as a mechanism for Fe isotope fractionation during dissimilatory iron oxide reduction. Environmental Science and Technology 39, 6698–6704.

Crosby, H.A., E.E. Roden, C.M. Johnson, and B.L. Beard (2007) The mechanism of iron isotope fractionation produced during dissimilatory Fe(III) reduction by *Shewanella putrefaciens* and *Geobacter sulfurreducens*. Geobiology 5, 169–189.

Dickens, G.R., M. Kölling, D.C. Smith, L. Schnieders, and the IODP Expedition 302 Scientists (2007) Rhizon sampling of pore waters on scientific drilling expeditions: An example from the IODP Expedition 302, Arctic Coring Expedition (ACEX). Proc. IODP Scientific Drilling 4, doi:10.22 04/iodp.sd.4.08.2007.

Egger M., O. Rasigraf, C.J. Sapart, T. Jilbert, M.S.M. Jetten, T. Röckmann, C. van der Veen, N. Bândă, B. Kartal, K.F. Ettwig, and C.P. Slomp (2015) Iron-mediated anaerobic oxidation of methane in brackish coastal sediments. Environmental Science and Technology 49, 277-283.

Ferdelman, T.G. (1988) The distribution of sulfur, iron, manganese, copper, and uranium in a salt marsh sediment core as determined by a sequential extraction method. Master thesis, University Delaware.

Guelke, M., F. von Blanckenburg, R. Schoenberg, M. Staubwasser, and H. Stuetzel (2010) Determining the stable Fe isotope signature of plant-available iron in soils. Chemical Geology 277, 269–280.

Guilbaud, R., I.B. Butler, and R.M. Ellam (2013) Abiotic pyrite formation produces a large Fe isotope fractionation. Science 332, 1548–1551.

Haese, R.R. (2006) The Biogeochemistry of Iron. In: Schulz H.D., Zabel, M. (editors) Marine Geochemistry. Berlin, Springer-Verlag, 207–240.

Haese, R.R., K. Wallmann, A. Dahmke, U. Kretzmann, P.J. Müller and H.D. Schulz (1997) Iron species determination to investigate early diagenetic reactivity in marine sediments. Geochimica et Cosmochimica Acta 61(1), 63–72.

Hebbeln, D., C. Scheurle, and F. Lamy (2003) Depositional history of the Helgoland mud area, German Bight, North Sea. Geo-Marine Letters 23, 81–90.

Henkel, S., J.M. Mogollón, Kerstin Nöthen, C. Franke, K. Bogus, E. Robin, A. Bahr, M. Blumenberg, T. Pape, R. Seifert, C. März, G.J. de Lange, and S. Kasten (2012) Diagenetic barium cycling in Black Sea sediments – A case study for anoxic marine environments. Geochimica et Cosmochimica Acta 88, 88–105.

Hertweck, G. (1983) Das Schlickgebiet in der inneren Deutschen Bucht. Aufnahme mit dem Sedimentechographen. Senckenbergiana marit 15, 219–249.

Homoky, W.B., S. Severmann, R.A. Mills, P.J. Statham, and G.R. Fones (2009) Pore-fluid Fe isotopes reflect the extent of benthic Fe redox recycling: Evidence from continental shelf and deep-sea sediments. Geology, 37(8), 751–754.

Homoky, W.B., S.G. John, T.M. Conway, and R.A. Mills (2013) Distinct iron isotopic signatures and supply from marine sediment dissolution. Nature Communications, 4:2143.

Huerta-Diaz, M. and J.W. Morse (1990) A quantitative method for determination of trace metal concentrations in sedimentary pyrite. Marine Chemistry 29, 119–144.

Hyacinthe, C. and P. van Cappellen (2004) An authigenic iron phosphate phase in estuarine sediments: composition, formation and chemical reactivity. Marine Chemistry 91, 227–251.

Jensen, M.M., B. Thamdrup, S. Rysgaard, M. Holmer, and H. Fossing (2003) Rates and regulation of microbial iron reduction in sediments of Baltic-North Sea transition. Biogeochemistry 65, 295–317.

Johnson, C.M, B.L. Beard, and E.E. Roden (2008) The iron isotope fingerprints of redox and biogeochemical cycling in modern and ancient Earth. Annual Review of Earth and Planetary Sciences 36, 457–493.

Kasten, S., T. Freudenthal, F.X. Gingele, and H.D. Schulz (1998) Simultaneous formation of iron-rich layers at different redox boundaries in sediments of the Amazon deep-sea fan Geochimica et Cosmochimica Acta 62(13), 2253–2264.

Kostka, J.E. and G.W. Luther (1994) Partitioning and speciation of solid iron in saltmarsh sediments. Geochimica et Cosmochimica Acta 58, 1701–1710.

Lohan, M.C., A.M. Aguilar-Islas, R.P. Franks and K.W. Bruland (2005) Determination of iron and copper in seawater at pH 1.7 with a new commercially available chelating resin, NTA Superflow. Analytica Chimica Acta 530, 121–129.

Lord III, C.J. (1980) The chemistry and cycling of iron, manganese and sulfur in a salt marsh sediment, Dissertation thesis, University of Delaware.

März, C., J. Hoffmann, U. Bleil, G.J. de Lange, and S. Kasten (2008) Diagenetic changes of magnetic and geochemical signals by anaerobic methane oxidation in sediments of the Zambezi deep-sea fan (SW Indian Ocean). Marine Geology 255, 118-130.

McKeague, J.A. and J.H. Day (1966) Dithionite- and oxalate-extractable Fe and Al as aids in differentiating various classes of soils. Canadian Journal of Soil Science 46, 13–22.

Mehra, O.P. and M.L. Jackson (1960) Iron oxide removal from soils and clays by a dithionite-citrate system buffered with sodium bicarbonate. 7th National Conference on Clays and Clay Minerals, 317–327.

Mikutta, C., J.G. Wiederhold, O.A. Cirpka, T.B. Hofstetter, B. Bourdon, U. von Gunten (2009) Iron isotope fractionation and atom exchange during sorption of ferrous iron to mineral surfaces. Geochimica et Cosmochimica Acta 73, 1795–1812.

Oni, O., T. Miyatake, S. Kasten, T. Richter-Heitmann, D. Fischer, L. Wagenknecht, A. Kulkarni, M. Blumers, S.I. Shylin, V. Ksenofontov, B.F.O. Costa, G. Klingelhöfer, and M.W. Friedrich (2015) Distinct microbial populations are tightly linked to the profile of dissolved iron in the methanic sediments of the Helgoland mud area, North Sea. Frontiers in Microbiology, doi: 10.3389/fmicb.2015.0036.

Phillips, E.J.P. and D.R. Lovley (1987) Determination of Fe(III) and Fe(II) in oxalate extracts of sediment. Soil Science Society of America Journal 51, 938–941.

Poulton, S.W. (2003) Sulfide oxidation and iron dissolution kinetics during the reaction of dissolved sulfide with ferrihydrite. Chemical Geology 202, 79-94.

Poulton, S.W., M.D. Krom, and R. Raiswell. (2004) A revised scheme for the reactivity of iron (oxyhydr)oxide mineral towards dissolved sulfide. Geochimica et Cosmochimica Acta 68, 3703–3715.

Poulton, S.W. and D.E. Canfield (2005) Development of a sequential extraction procedure for iron: implications for iron partitioning in continentally derived particulates. Chemical Geology 214, 209–221.

Poulton, S.W. and D.E. Canfield (2011) Ferruginous conditions: A dominant feature of the ocean through Earth's history. Elements 7(2), 107–112.

Raiswell, R., D.E. Canfield, and R.A. Berner (1994) A comparison of iron extraction methods for the determination of degree of pyritisation and the recognition of iron-limited pyrite formation. Chemical Geology 111, 101–110.

Raiswell, R., H.P. Vu, L. Brinza, L.G. Benning (2010) The determination of labile Fe in ferrihydrite by ascorbic acid extraction: methodology, dissolution kinetics and loss of solubility with age and de-watering. Chemical Geology 278, 70-79.

Raiswell and Canfield (2012) The iron biogeochemical cycle past and present. Geochemical Perspectives 1(1).

Riedinger, N., K. Pfeifer, S. Kasten, J.F.L. Garming, C. Vogt, and C. Hensen (2005) Diagenetic alteration of magnetic signals by anaerobic oxidation of methane related to a change in sedimentation rate. Geochimica et Cosmochimica Acta 69(16), 4117–4126.

Riedinger N., M.J. Formolo, T.W. Lyons, S. Henkel, A. Beck, and S. Kasten (2014) An inorganic geochemical argument for coupled anaerobic oxidation of methane and iron reduction in marine sediments. Geobiology 12, 172−181.

Schoenberg, R. and von F. Blanckenburg (2005), An assessment of the accuracy of stable Fe isotope ratio measurements on samples with organic and inorganic matrices by high-resolution multicollector ICP-MS. International Journal of Mass Spectrometry 242, 257–272.

Scholz, F., S. Severmann, J. McManus, A. Noffke, U. Lomnitz, and C. Hensen (2014) On the isotope composition of reactive iron in marine sediments: Redox shuttle versus early diagenesis. Chemical Geology 389, 48–59.

Schwertmann, U. (1964) Differenzierung der Eisenoxide des Bodens durch photochemische Extraktion mit saurer Ammoniumoxalat-Lösung. Zeitschrift zur Pflanzenernährung und Bodenkunde, 195, 194–202.

Seeberg-Elverfeldt, J., M. Schlüter, T. Feseker and M. Kölling (2005), Rhizon sampling of porewaters near the sediment-water interface of aquatic systems. Limnology and Oceanography: Methods 3, 361–371.

Segarra, K.E.A., C. Comerford, J. Slaughter, and S.B. Joye (2013). Impact of electron acceptor availability on the anaerobic oxidation of methane in coastal freshwater and brackish wetland sediments. Geochimica et Cosmochimica Acta 115, 15–30.

Severmann, S., C.M. Johnson, B.L. Beard, and J. McManus (2006) The effect of early diagenesis on the Fe isotope compositions of porewaters and authigenic minerals in continental margin sediments. Geochimica et Cosmochimica Acta 70, 2006–2022.

Severmann, S., J. McManus, W.M. Berelson, and D.E. Hammond (2010) The continental shelf benthic iron flux and its isotope composition. Geochimica et Cosmochimica Acta, 74, 3984–4004.

Sivan, O., M. Adler, A. Pearson, F. Gelman, I. Bar-Or, S.G. John, and W. Eckerte (2011) Geochemical evidence for iron-mediated anaerobic oxidation of methane. Limnology and Oceanography, 56(4), 1536–1544.

Sivan, O., G. Antler, A.V. Turchyn, J.J. Marlow, and V.J. Orphan (2014) Iron oxides stimulate sulfate-driven anaerobic methane oxidation in seeps. Proceedings of the National Academy of Sciences of the United States of America, 1−9.

Slomp, C.P., J.F.P. Malschaert, L. Lohse, and W. Van Raaphorst (1997) Iron and manganese cycling in different sedimentary environments on the North Sea continental margin. Continental Shelf Research 17(9), 1083-1117.

Staubwasser, M., F. v. Blanckenburg, and R. Schoenberg (2006) Iron isotopes in the early marine diagenetic iron cycle. Geology 34, 629–632.

Staubwasser, M., R. Schoenberg, F. von Blanckenburg, S. Krüger, and C. Pohl (2013) Isotope fractionation between dissolved and suspended particulate Fe in the oxic and anoxic water column of the Baltic Sea. Biogeosciences 10, 233–245.

Stookey, L. (1970) Ferrozine – A new spectrophotometric reagent for iron. Analytical Chemistry 42(7), 779 –781.

Strelow, F.W.E. (1980) Improved separation of iron from copper and other elements by anion-exchange chromatography on a 4% cross-linkage resin with high concentrations of hydrochloric acid. Talanta 27, 727–732.

Stucki, J.W., B.A. Goodman, and U. Schwertmann (Eds) (1988) Iron in soils and clay minerals. D. Reidel, Dordrecht, the Netherlands.

Tessier, A., P.G.C. Campbell, M. Bisson, (1979) Sequential extraction procedure for the speciation of particulate trace metals. Analytical Chemistry 51, 844–851.

Wiederhold, J.G., N. Teutsch, S.M. Kraemer, A.N. Halliday, and R. Kretschmar (2007a) Iron isotope fractionation during pedogenesis in redoximorphic soils. Soil Science Society of America Journal 71(6), 1840–1850.

Wiederhold, J.G., N. Teutsch, S.M. Kraemer, A.N. Halliday, and R. Kretzschmar (2007b) Iron isotope fractionation in oxic soils by mineral weathering and podsolization. Geochimica et Cosmochimica Acta 71 (23), 5821–5833.

Wiesli, R.A., B.L. Beard, and C.M. Johnson (2004) Experimental determination of Fe isotope fractionation between aqueous Fe(II), siderite and “green rust” in abiotic systems. Chemical Geology 211, 343–362.

Williams, A.G.B. and M.M. Scherer (2004) Spectroscopic evidence for Fe(II)-Fe(III) electron transfer at the iron oxide-water interface. Environmental Science and Technology 38, 4782–4790.

Wu, L., B.L. Beard, E.E. Roden, and C.M. Johnson (2011) Stable iron isotope fractionation between aqueous Fe(II) and hydrous ferric oxide. Environmental Science and Technology 45, 1847–1852.

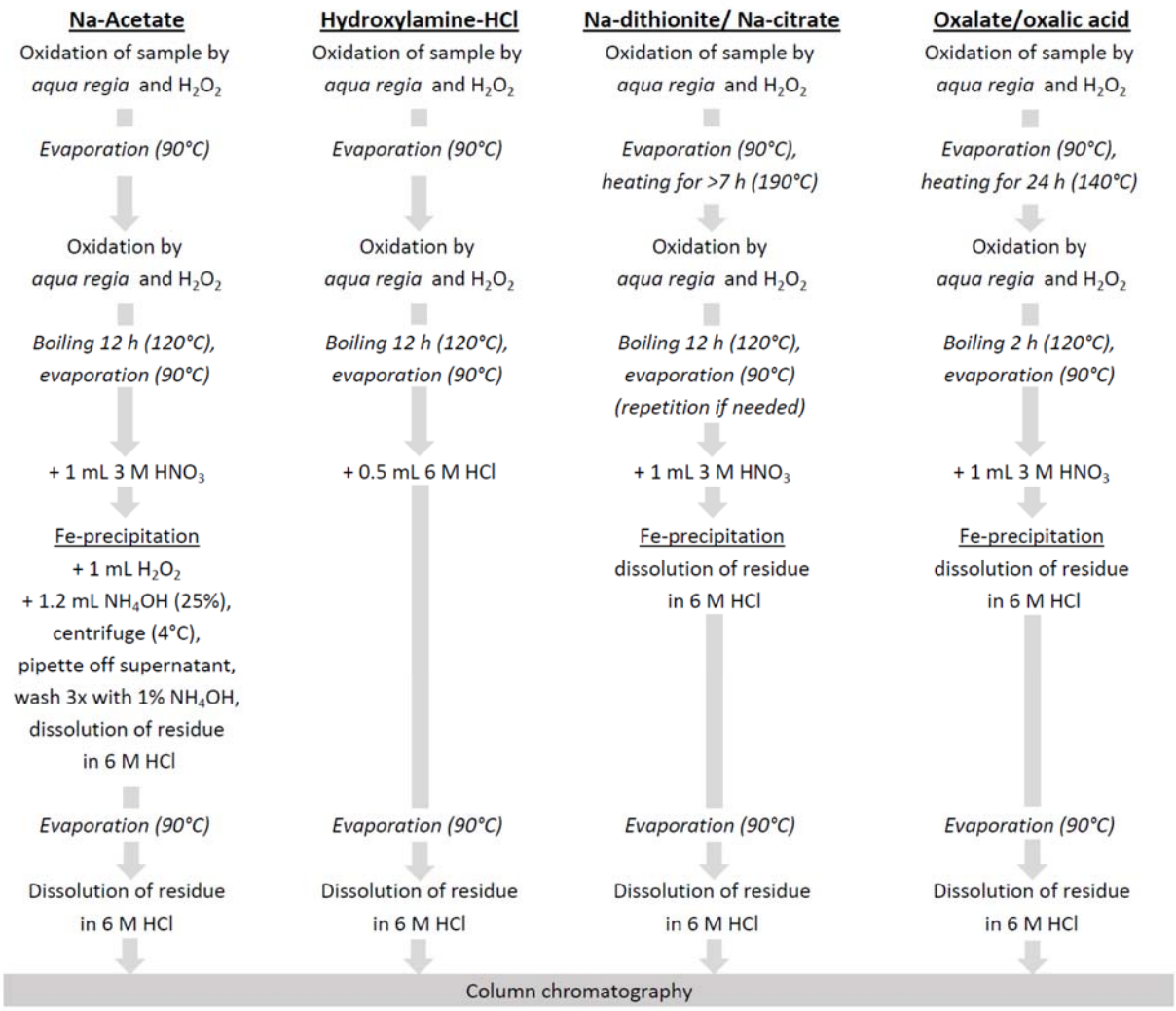

Fig. 1: Chemical processing of iron extracts for Fe isotope analysis.

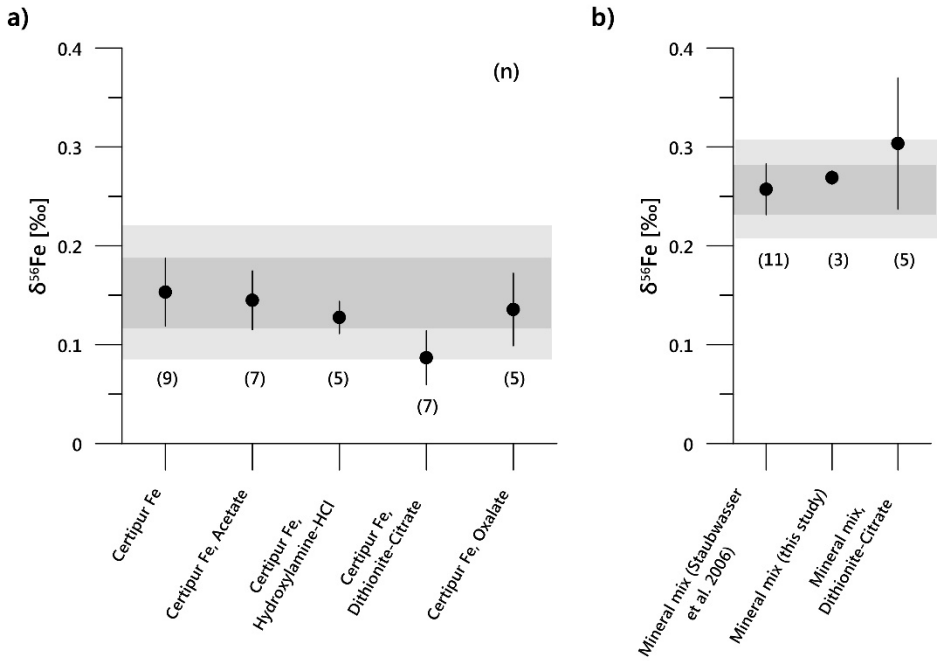

Fig. 2: Isotope data (δ^{56}Fe) of a) the Certipur® Fe solution without addition of leaching reagents and chemical processing (mineral mix, Certipur® Fe) and after addition of reagents and subsequent purification and b) of the mineral mix standard. Error bars are the standard deviation (1SD). The light greyish area indicates 2SD of the reference standard.

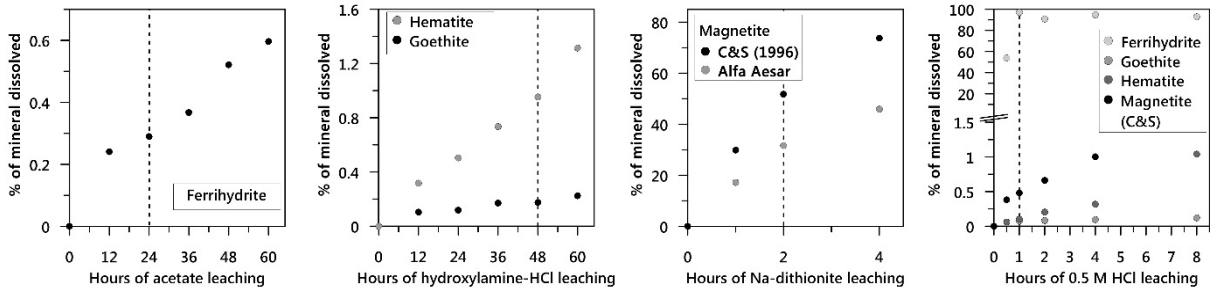

Fig. 3: Dissolution of non-target minerals by chemical treatment with acetate, hydroxylamine-HCl, Na-dithionite and dissolution of target (ferrihydrite) and non-target minerals (goethite, hematite, and magnetite) by 0.5 M HCl. The dashed lines indicate optimum extraction times for sediment samples at room temperature as given by Poulton and Canfield (2005) and Kostka and Luther (1994), respectively. Tests with dithionite were performed with magnetite synthesized after Cornell and Schwertmann (1996) and purchased from Alfa Aesar.

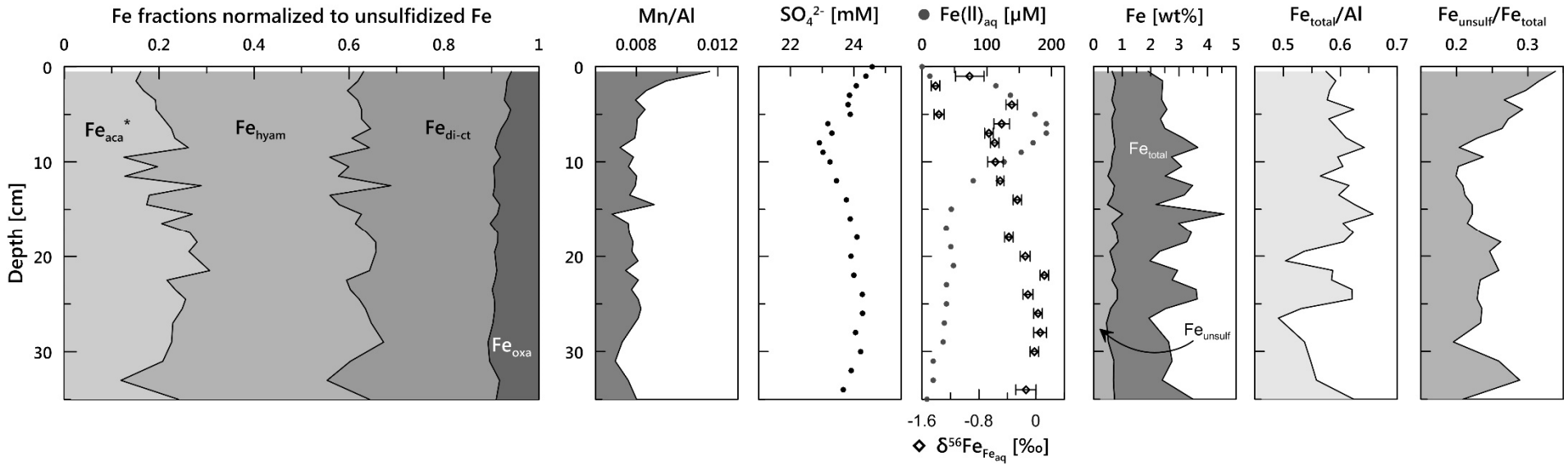

Fig. 4: Chemical data to site HE337-1 including sequentially leached Fe fractions normalized to unsulfidized reactive Fe (Fe_{unsulf} = Fe_{aca}* + Fe_{hyam} + $Fe_{di\text{-}ct}$ + Fe_{oxa}), Mn/Al, pore-water SO_4^{2-}, $Fe(II)_{aq}$, $\delta^{56}Fe_{Fe_{aq}}$, Fe_{total} and Fe_{react}, Fe_{total}/Al, and Fe_{react}/ Fe_{total}. Solid phase and pore-water data were gained for parallel cores. Fe_{aca}* was corrected for Fe_{AVS}.

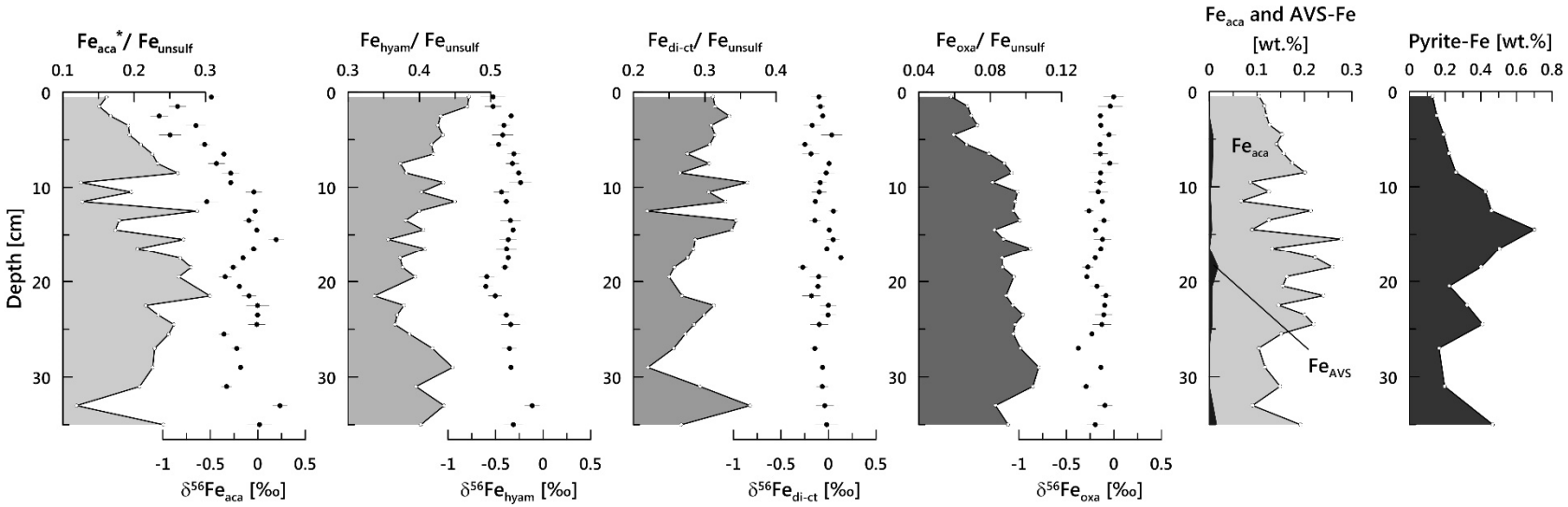

Fig. 5: Sequentially extracted Fe fractions normalized to reactive Fe and respective δ56Fe for core location HE337-1. Graphs on the left side show AVS- and pyrite-Fe as determined after Canfield et al. (1986). Fe_{aca}* was corrected for Fe_{AVS}. Isotopic data is also shown in Table A.5.

779 Table 1: Recoveries of Certipur® Fe standard and blanks after addition and removal of extraction
780 solutions and column separation. Recoveries of Fe were normalized to standards that were processed
781 without addition of extraction reagents and chemical processing.

Extractant	Recovery of Fe (%)	n	Fe present in blanks (µg)	n
Na-Acetate	101.1 ± 1.2	6	0.2 ± 0.2	7
Hydroxylamine-HCl	101.4 ± 0.8	5	0.4 ± 0.1	9
Na-dithionite-citrate	97.5 ± 0.8	5	0.4 ± 0.4	7
Oxalate/ oxalic acid	82.9 ± 12.9	5	0.1 ± 0.1	6

782

783

784 Table 2: Selectivity of extraction steps as tested by treatment of pairs of 58Fe non-spiked and spiked
785 minerals. Isotopic ratios of mixtures and end-members are given in A.1 and A.2. C&S: magnetite
786 synthesized after Cornell and Schwertmann (1996); AA: magnetite purchased from Alfa Aesar.

Non-spiked mineral	Spiked mineral	Extractant and duration	n	Fe from mineral (in % of total dissolved Fe)		% of mineral dissolved	
				Non-spiked mineral	Spiked mineral	Non-spiked mineral	Spiked mineral
Ferrihydrite*	Goethite	Hydrox.-HCl, 48 h	3	98.5 ± 0.2	1.5 ± 0.2	87.5 ± 0.7	0.9 ± 0.3
Ferrihydrite*	Hematite	Hydrox.-HCl, 48 h	3	97.6 ± 0.6	2.4 ± 0.6	86.4 ± 1.8	1.3 ± 0.2
Goethite*	Magnetite (C&S)	Dith., 2 h	3	51.2 ± 3.5	48.8 ± 3.5	96.3 ± 3.0	74.3 ± 1.5
Hematite*	Magnetite (C&S)	Dith., 2 h	3	58.7 ± 11.0	41.3 ± 11.0	95.5 ± 9.2	63.1 ± 19.4
Magnetite (AA)	Goethite*	Dith., 2 h	2	37.4 ± 3.6	62.6 ± 3.6	33.5 ± 3.9	78.5 ± 9.6
Magnetite (AA)	Hematite*	Dith., 2 h	3	34.0 ± 3.6	67.0 ± 4.5	34.1 ± 0.9	88.0 ± 1.5

*target mineral

787